Numerical simulation of counter-current liquid–liquid extraction for recovering Co, Ni and Li from lithium-ion battery leachates of varying composition

Vasilyev Fedor, Virolainen Sami, Sainio Tuomo

DOI: 10.1016/j.seppur.2018.08.036

Separation and Purification Technology 210 (2019) 530–540

Contents lists available at ScienceDirect

Separation and Purification Technology

journal homepage: www.elsevier.com/locate/seppur

Numerical simulation of counter-current liquid–liquid extraction for recovering Co, Ni and Li from lithium-ion battery leachates of varying composition

Fedor Vasilyev, Sami Virolainen, Tuomo Sainio*

Lappeenranta University of Technology, School of Engineering Science, P.O. Box 20, FI-53851 Lappeenranta, Finland

ARTICLE INFO

Keywords:
Liquid–liquid extraction
Li-ion battery waste
Process design
Continuous counter-current operation
Nonlinear regression

ABSTRACT

Fractionation of Li-ion battery waste leachates into high-purity Li, Ni, and Co streams in a liquid − liquid extraction circuit was studied using numerical simulations. A new mechanistic mathematical model explaining the phase equilibrium in the loading, scrubbing, and stripping stages using bis(2,4,4-trimethylpentyl)phosphinic acid (Cyanex 272) as extractant was developed. Including the distribution equilibrium of ammonia in the model enabled simulation of metal extraction with partially neutralized extractant. The model facilitates the design and optimization of liquid–liquid extraction circuit for fractionation of Li-ion battery leachates. Four leachates from recent research articles were selected to the study in order to cover a wide composition variation. In the separation process scheme studied, Co and Ni are first selectively extracted, yielding a pure Li raffinate, and then separated as pure products in the stripping steps. The simulation results confirm the viability of the scheme. The influence of the leachate composition on the feasible range of O/A ratios in loading and scrubbing as well as acid concentration in Ni stripping was quantified. With proper operating parameters, high recoveries of Li and Co (> 99.9%) are achieved for all leachate compositions. The leachates containing 10–25 g/L Co, > 10 g/L Ni, and > 2.5 g/L Li are particularly suitable for fractionation of the metals into high-purity (> 99%) Li, Ni, and Co streams.

1. Introduction

Li-ion batteries are widely used for powering portable electronic devices of different types due to the favorable properties of Li, which has the highest redox potential value, and the highest specific heat capacity, of any solid element [1]. Currently, Li-ion batteries account for 37% of all the rechargeable batteries produced in the world, and their share is increasing. The number of appliances powered by this type of battery is growing as well. In total, 39% of produced Li is consumed in the manufacture of batteries [1]. Moreover, a sharp increase in Li demand is expected in the near future, due to the rapid development of the electric vehicle market [2,3].

Along with Li, spent Li-ion batteries contain hazardous materials; Co is classified as critical, and others are extensively used base metals (Mn, Ni, Cu, *etc.*) [2]. As the estimated operational life of Li-ion batteries is 10 years, the amount of these metals available from spent batteries, as a secondary resource, will only increase, along with an increase in the number of batteries in use [4]. Therefore, the investigation of processes for recovery and recycling of metals from spent batteries has become highly desirable, from both environmental and economic viewpoints [2,5].

In a hydrometallurgical process applied for the recovery of valuable metals from spent Li-ion batteries, the battery waste is usually leached with H_2SO_4 or HCl acid [6,7] after mechanical and possibly some other pretreatment [8,9]. Also, H_3PO_4 was reported [10] to be a suitable agent for the leaching of the cathode materials ($LiCoO_2$) and Co recovery. In addition, some organic acids such as citric acid [11] were considered as a leaching agent. As mentioned above, along with Li, Ni, and Co, Li-ion batteries contain significant amounts of Cu (7–17%), Al (3–10%) and Fe (up to 20%) [12] that may also be leached. Cu, Al, Mn, and Fe can be removed from the leachate by precipitation [13,14], or liquid − liquid extraction with 2-hydroxy-5-nonylsalicylaldoxime (Acorga M5640) [5], leaving Li, Ni, and Co in the solution. The utilization of the hydroxyoxime reagent also allows recovery of pure Cu.

Organophosphorus reagents bis(2,4,4-trimethylpentyl)phosphinic acid (Cyanex 272, Mextral 272P, P507) and 2-ethylhexyl hydrogen(2-ethylhexyl)phosphate (PC-88A) are solely used for separation of Co, Ni, and Li due to their good Co/Ni selectivity and low extractability of Li

* Corresponding author.
E-mail address: tuomo.sainio@lut.fi (T. Sainio).

https://doi.org/10.1016/j.seppur.2018.08.036
Received 17 April 2018; Received in revised form 8 August 2018; Accepted 21 August 2018
Available online 23 August 2018

Nomenclature

Abbreviations

LLX	liquid–liquid extraction
SSR	sum of the squared residuals

Letters

A	deprotonated phosphinic acid
a	activity
c	molar concentration
E	extent of extraction
HA	protonated phosphinic acid
I	ionic strength
k	reaction rate constant
K	equilibrium constant
M	extractable cations Co^{2+}, Ni^{2+}, Li^{+}, or NH_4^{+}
R	rate of an elementary reaction
S	number of reactions in the system

Greek

γ	activity coefficient
ϑ	stoichiometric coefficient of the species
σ	standard deviation of the parameter estimates

Subscripts and superscripts

Aq	aqueous phase
exp	measured experimental data
f	forward
mod	data calculated with model
Org	organic phase
r	reverse

from acidic solutions [6]. The separation of Co and Ni is a well-studied application of liquid − liquid extraction in hydrometallurgy [15]. The plants that use liquid − liquid extraction for Co/Ni separation process solutions resulting from ores, concentrates, precipitates, matte, various scrap materials, and waste effluents [16], operate mostly with di(2,4,4′-trimethylpentyl)phosphinic acid (Cyanex 272, Mextral 272P, P507). The active component has been shown to yield high selectivity, low aqueous phase solubility, and high chemical stability [15]. Virolainen et al. [6] showed that high Co/Ni selectivity of Cyanex 272 makes this extractant a more attractive choice than PC-88A for the fractionation of Co, Ni, and Li.

In response to the increasing necessity to recycle spent Li-ion batteries, a number of studies have suggested employing liquid–liquid extraction to recover and separate Co, Ni, and Li from battery leachates [3,5,6,11]. A challenge for utilization of the phase equilibrium and pilot data available in the literature is that the composition of the leachate may vary strongly depending on the exact Li-ion battery chemistry and leaching conditions. To the authors' knowledge, the influence of Li battery leachate composition on the performance and operation of continuous counter-current liquid–liquid extraction processes has not been investigated.

Numerical simulation of extraction processes can aid in understanding the influence of different operation conditions on process performance. Yet, there are no detailed numerical modeling and simulation studies on the liquid − liquid extraction processes for Li-ion batteries recycling. Slope analysis is often used for determining the nature of the extracted complexes and the stoichiometry of the metal extraction reactions [5,17–20]. Process design usually relies on McCabe-Thiele analysis, which is used for determination of the number of theoretical stages required in loading, scrubbing, and stripping steps to achieve a specified purification and recovery in a counter-current operation [18,20–22]. The method heavily relies on extraction equilibrium data in the form of loading, scrubbing, and stripping isotherms, which are different for different extractant concentrations and acidity of aqueous phase. Moreover, it is best suited for designing single metal extraction and does not give a good indication of the impurity transfer in the process. Bourget et al. [23] introduced a simulation software that relies on the simultaneous solution of multiple equilibrium calculations based on pre-generated equilibrium data. The capabilities of the simulation tool were demonstrated in optimization of the design parameters of a circuit for recovery of Ni and Co. Even though the modeling method allows for transfer of impurities, it requires large variations in the experimental data to predict process performance accurately over a wide range of operating conditions. Alternatively, mechanistic modeling offers higher flexibility and accuracy in process simulation and design [24,25], especially in systems with competitive extraction reactions. Calibration of the models with reasonable amount of experimental data is however still required.

An effective Li-ion battery leachate fractionation process was earlier proposed by Virolainen et al. [6] and demonstrated in continuous counter-current runs for loading, scrubbing and stripping steps individually. However, the operation of the entire process was not validated. The process focuses on the separation of Co, Ni, and Li, which is the final stage in the processing of Li-ion battery leachate when all the other impurities (*e.g.* Cu, Al, Mn, and Fe) are removed by either selective precipitation or liquid–liquid extraction.

The objective of this study was to examine by numerical simulations the operation of the entire process scheme proposed by Virolainen et al. [6] in application to fractionation of Li-ion battery leachates of different compositions. For this purpose, a new mechanistic mathematical model of the equilibrium liquid–liquid extraction of Li, Co, and Ni with Cyanex 272 extractant from a sulfate solution was developed. The removal of other impurities in the initial stages of the Li-ion battery leachates processing is not considered because there are several known solutions discussed above. The same process scheme was studied for fractionation of four different Li-ion battery leachates presented in the literature [6,21,26,27]. The four leachates differed significantly in the target metals concentrations (Co, Ni, and Li). For three leachates [21,26,27], different process flowsheets have been originally suggested but the designs have not been verified by continuous experimental runs or simulations. It is shown here that numerical simulations can be used for optimization of the entire process and for analysis of process operation limitations over a wide range of feed concentrations.

2. Modeling

In the current study, the liquid–liquid extraction of Co, Ni, and Li is considered to be an interphase extraction process (Fig. 1). The extraction equilibrium is modeled by taking into account the aqueous phase speciation, the competing interfacial ion exchange extraction reactions of the cations, and the formation of extracted cation-extractant complexes of different stoichiometries in the bulk organic phase.

Acidic organophosphorus extractants are frequently used in the form of their Na or ammonium salts in order to facilitate pH control of the operations when the leaching solutions contain high concentrations (> 3 g/L) of the metals being extracted [28–30]. Hence, it is important to study, in addition to the extraction behavior of the metal ions, also the extraction of ammonia [30]. Yet, up to now, no model has been suggested that could describe the ammonia equilibrium distribution in the range of pH 2–7, corresponding to the loading and stripping steps in

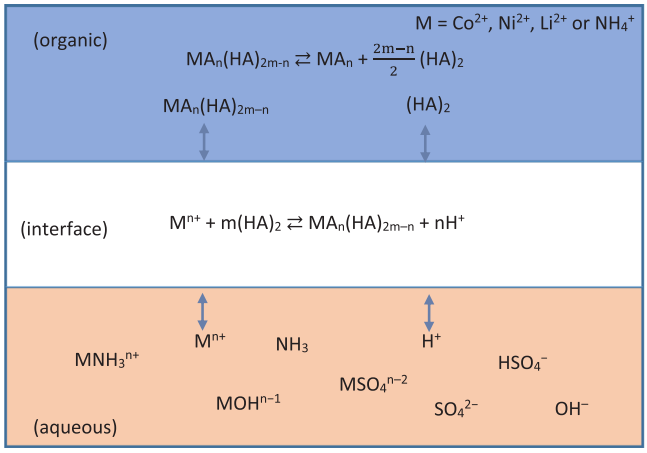

Fig. 1. Mechanism of the liquid – liquid extraction of Li, Ni, and Co from a sulfate solution with saponified phosphinic acid in an aqueous/organic two-phase system. M stands for extractable cations Co^{2+}, Ni^{2+}, Li^{+}, or NH_4^{+}; A stands for deprotonated phosphinic acid.

the process of liquid – liquid separation of Co and Ni. The liquid – liquid equilibrium distribution of ammonia is thus accounted for here.

2.1. Extraction of Co, Ni, and Li

2.1.1. Aqueous phase speciation

The aqueous phase in liquid–liquid extraction contains ions that are products of the dissociation reactions listed in Table 1. The corresponding equations for the equilibrium constants (Eqs. (1–18)) are also listed in Table 1. The values of the equilibrium constants were taken from the database of Medusa software [31]. The value of the equilibrium constant for sulfuric acid in Eq. (1) was set to be small ($\log K = -3$) to represent complete dissociation [25]. The hydrolysis reactions of Co and Ni were included in the speciation model because the operation of some steps in the process considered herein is intended to be around pH 7, where precipitation of the metal hydroxides is possible (but of course undesirable). The equilibrium constants of the hydrolysis reactions listed in Table 1 include the concentration of water, which was assumed to be constant.

In concentrated aqueous solutions, electrolyte speciation can be determined using appropriate reaction equilibrium constants and ionic activity coefficient models, derived from the Debye–Hückel theory [25,32]. The extended Debye–Hückel model, Eq. (19), was used herein to calculate activity coefficients for the aqueous phase species. A discussion on the model is presented elsewhere [24,25,32]. The activity coefficient γ relates the activity a to a measured molar concentration for the species in the aqueous phase: $a = \gamma c$. Activity coefficients of the species in the organic phase were assumed unity.

$$\log\gamma_i = \frac{-Az_i^2\sqrt{I}}{1 + \mathring{a}_i B\sqrt{I}} + \dot{B}I \tag{19}$$

where $\mathring{a}_i$ is the hard-core diameter of the i-th ionic species, z_i is the charge of the i-th species, A and B are the Debye–Hückel parameters, and I is the ionic strength of the electrolyte solution.

2.1.2. Extraction mechanism

Depending on the extraction conditions, organophosphorus acid-based extractants are known to form complexes of variable stoichiometry with metal ions. These complexes are preferentially distributed into the organic phase [18–20,28]. The extractant-to-metal molar ratio for divalent metal ions changes from four (tetrahedral complex) to two (polymer formation), as the loading of the organic phase increases and less extractant molecules are available for metal complexation [29]. The liquid–liquid extraction of a given divalent metal by an organophosphorus acid-based extractant can be described assuming two stepwise reactions [33,34], the first one of which is an ion transfer at the interface of the aqueous and organic phases, where M stands for Co or Ni:

$$M^{2+} + 2\overline{(HA)_2} \rightleftarrows \overline{MA_2(HA)_2} + 2H^+ \tag{20}$$

and the second of which occurs in the bulk organic phase as a breakdown of the complex $MA_2(HA)_2$:

$$\overline{MA_2(HA)_2} \rightleftarrows \overline{MA_2} + \overline{(HA)_2} \tag{21}$$

In the case of Co and Ni, the first extraction reaction step takes the form shown in Eqs. (22) and (24), which leads to the expression of the extraction equilibrium constants, Eqs. (23) and (25):

$$Co^{2+} + 2\overline{(HA)_2} \rightleftarrows \overline{CoA_2(HA)_2} + 2H^+ \tag{22}$$

$$K_{LLX,1}^{Co} = \frac{a(\overline{CoA_2(HA)_2})\cdot a(H^+)^2}{a(Co^{2+})\cdot a(\overline{(HA)_2})^2} \tag{23}$$

$$Ni^{2+} + 2\overline{(HA)_2} \rightleftarrows \overline{NiA_2(HA)_2} + 2H^+ \tag{24}$$

$$K_{LLX,1}^{Ni} = \frac{a(\overline{NiA_2(HA)_2})\cdot a(H^+)^2}{a(Ni^{2+})\cdot a(\overline{(HA)_2})^2} \tag{25}$$

At high organic loading, the breakdown of the extracted complexes of Co and Ni in the bulk organic phase is described by Eqs. (26) and (28) that lead to the expression of the extraction equilibrium constants, Eqs. (27) and (29):

$$\overline{CoA_2(HA)_2} \rightleftarrows \overline{CoA_2} + \overline{(HA)_2} \tag{26}$$

Table 1
Aqueous speciation reactions included in the model for aqueous phase speciation in the simulated sulfate leachate of Li-ion battery waste [25,31]. Equilibrium constants of the hydrolysis reactions include the concentration of water, which was assumed to be constant.

Chemical reaction	Equation for equilibrium constant	log$K$	
$H^+ + HSO_4^- \rightleftarrows H_2SO_4$	$K_1 = \frac{a(H_2SO_4)}{a(H^+)\cdot a(HSO_4^-)}$	−3	(1)
$H^+ + SO_4^{2-} \rightleftarrows HSO_4^-$	$K_2 = \frac{a(HSO_4^-)}{a(H^+)\cdot a(SO_4^{2-})}$	1.98	(2)
$Co^{2+} + SO_4^{2-} \rightleftarrows CoSO_4$	$K_3 = \frac{a(CoSO_4)}{a(Co^{2+})\cdot a(SO_4^{2-})}$	2.34	(3)
$Co^{2+} + H_2O \rightleftarrows H^+ + CoOH^-$	$K_4 = \frac{a(CoOH^-)\cdot a(H^+)}{a(Co^{2+})}$	−9.2	(4)
$Co^{2+} + H_2O \rightleftarrows 2H^+ + Co(OH)_2$	$K_5 = \frac{a(Co(OH)_2)\cdot a(H^+)^2}{a(Co^{2+})}$	−18.6	(5)
$Co^{2+} + H_2O \rightleftarrows 2H^+ + Co(OH)_{2,s}$	$K_6 = \frac{a(H^+)^2}{a(Co^{2+})}$	−12.2	(6)
$Co^{2+} + NH_3 \rightleftarrows CoNH_3^{2+}$	$K_7 = \frac{a(CoNH_3^{2+})}{a(Co^{2+})\cdot a(NH_3)}$	2.1	(7)
$Ni^{2+} + SO_4^{2-} \rightleftarrows NiSO_4$	$K_8 = \frac{a(NiSO_4)}{a(Ni^{2+})\cdot a(SO_4^{2-})}$	2.29	(8)
$Ni^{2+} + H_2O \rightleftarrows H^+ + NiOH^-$	$K_9 = \frac{a(NiOH^-)\cdot a(H^+)}{a(Ni^{2+})}$	−9.5	(9)
$Ni^{2+} + H_2O \rightleftarrows 2H^+ + Ni(OH)_2$	$K_{10} = \frac{a(Ni(OH)_2)\cdot a(H^+)^2}{a(Ni^{2+})}$	−20.01	(10)
$Ni^{2+} + H_2O \rightleftarrows 2H^+ + Ni(OH)_{2,S}$	$K_{11} = \frac{a(H^+)^2}{a(Ni^{2+})}$	−10.5	(11)
$Ni^{2+} + NH_3 \rightleftarrows NiNH_3^{2+}$	$K_{12} = \frac{a(NiNH_3^{2+})}{a(Ni^{2+})\cdot a(NH_3)}$	2.73	(12)
$Li^+ + SO_4^{2-} \rightleftarrows LiSO_4^-$	$K_{13} = \frac{a(LiSO_4^-)}{a(Li^+)\cdot a(SO_4^{2-})}$	2.29	(13)
$Li^+ + H_2O \rightleftarrows H^+ + LiOH$	$K_{14} = \frac{a(LiOH)\cdot a(H^+)}{a(Li^+)}$	−9.5	(14)
$Li^+ + NH_3 \rightleftarrows LiNH_3^+$	$K_{15} = \frac{a(LiNH_3^+)}{a(Li^+)\cdot a(NH_3)}$	−0.7	(15)
$H^+ + NH_3 \rightleftarrows NH_4^+$	$K_{16} = \frac{a(NH_4^+)}{a(H^+)\cdot a(NH_3)}$	9.237	(16)
$H^+ + NH_3 + SO_4^{2-} \rightleftarrows NH_4SO_4^-$	$K_{17} = \frac{a(NH_4SO_4^-)}{a(H^+)\cdot a(NH_3)\cdot a(SO_4^{2-})}$	9.237	(17)
$H_2O \rightleftarrows H^+ + OH^-$	$K_{18} = a(H^+)\cdot a(OH^-)$	−14	(18)

$$K_{LLX,2}^{Co} = \frac{a(\overline{CoA_2})\cdot a(\overline{(HA)_2})}{a(\overline{CoA_2(HA)_2})} \quad (27)$$

$$\overline{NiA_2(HA)_2} \rightleftarrows \overline{NiA_2} + \overline{(HA)_2} \quad (28)$$

$$K_{LLX,2}^{Ni} = \frac{a(\overline{NiA_2})\cdot a(\overline{(HA)_2})}{a(\overline{NiA_2(HA)_2})} \quad (29)$$

Li is extracted by Cyanex 272 at lower acidity in comparison to cobalt and nickel. Under such conditions, the organic phase is assumed to be loaded, to a high degree, by Co and Ni, and extraction of Li is possible with only one dimeric extractant molecule according to the reaction in Eq. (30). This leads to the expression of the extraction equilibrium constant shown in Eq. (31).

$$Li^+ + \overline{(HA)_2} \rightleftarrows \overline{LiA\cdot HA} + H^+ \quad (30)$$

$$K_{LLX}^{Li} = \frac{a(\overline{LiA\cdot HA})\cdot a(H^+)}{a(Li^+)\cdot a(\overline{(HA)_2})} \quad (31)$$

As has already been discussed in the introduction, when leaching solutions contain high concentrations of the metals to be extracted, the extractant is used in the saponified form to reduce the generation of acid during the extraction. The reaction in Eq. (32) is usually used to describe the extraction mechanism of a divalent metal ion, with the pre-neutralized organophosphorus extractant, when slope analysis is employed [5,17,18]:

$$M^{2+} + \overline{(HA)_2} + 2\overline{NH_4A} \rightleftarrows \overline{MA_2(HA)_2} + 2NH_4^+ \quad (32)$$

The reaction explains how the pre-neutralization prevents excessive generation of acid in the loading step by means of exchange of the metal and ammonium ions. However, Eq. (32) gives only a qualitative explanation of the overall interfacial extraction mechanism, and is not suitable for the mechanistic modeling of the extraction equilibrium of Co, Ni, and Li. Therefore, a model of ammonia equilibrium distribution, developed in the next section, was included in the model for an extraction equilibrium of the metal ions.

2.1.3. Liquid–liquid distribution equilibrium of ammonia

Inoue et al. [30] studied the extraction of ammonium with Cyanex 272 and found that it is extracted as an ion-pair $NH_4A(HA)_4$, according to Eq. (33), in the low pH region (pH < 6), in which the loading of ammonia in the organic phase is low. The extraction equilibrium constant for the extraction reaction can be expressed in the form of Eq. (34). Also, it was concluded that ammonia exists as NH_4A complex in the organic phase in the region of the high loading ratio of ammonia to the extractant, at pH > 7 [30]; however, there have been no quantitative studies on its distribution equilibrium at pH 2–8 to date.

$$NH_4^+ + 2.5\overline{(HA)_2} \rightleftarrows \overline{NH_4A(HA)_4} + H^+ \quad (33)$$

$$K_{LLX}^{NH_4A(HA)_4} = \frac{a(\overline{NH_4A(HA)_4})\cdot a(H^+)}{a(NH_4^+)\cdot a(\overline{(HA)_2})^{2.5}} \quad (34)$$

Lindell et al. [28] studied the water (NH_3)/Cyanex 272/aliphatic diluent (D-70, Shell Chemicals) system and concluded that, at a high aqueous ammonia concentration, a single-phase microemulsion is formed at an ammonia/organic acid molar ratio of 1. The microemulsion contains reversed micelles enclosing the water. Upon contact with an acidic aqueous phase in the loading stage of the liquid − liquid extraction, the breakdown of the microemulsion is assumed here to follow the reaction in Eq. (35), which has an extraction equilibrium constant in the form of Eq. (36). The influence of the presence of water in the microemulsion on volume change was neglected.

$$2NH_4^+ + \overline{(HA)_2} \rightleftarrows 2\overline{NH_4A} + 2H^+ \quad (35)$$

$$K_{LLX}^{NH_4A} = \frac{a(\overline{NH_4A})^2\cdot a(H^+)^2}{a(NH_4^+)^2\cdot a(\overline{(HA)_2})} \quad (36)$$

Table 2
Aqueous speciation reactions in the liquid–liquid extraction of ammonia from an ammonium nitrate solution [31,35].

Chemical reaction	Equation for equilibrium constant	log*K*	
$NH_4^+ + NO_3^- \rightleftarrows NH_4NO_3$	$K_{19} = \frac{a(NH_4NO_3)}{a(NH_4^+)\cdot a(NO_3^-)}$	−1.63	(37)
$H^+ + NO_3^- \rightleftarrows HNO_3$	$K_{20} = \frac{a(HNO_3)}{a(H^+)\cdot a(NO_3^-)}$	−1.283	(38)
$H^+ + NH_3 \rightleftarrows NH_4^+$	$K_{21} = \frac{a(NH_4^+)}{a(H^+)\cdot a(NH_3)}$	9.237	(39)
$H_2O \rightleftarrows H^+ + OH^-$	$K_{22} = a(H^+)\cdot a(OH^-)$	−14	(40)

The reaction in Eq. (32) is actually obtained by combining the reactions in Eqs. (20) and (35). Therefore, Eq. (32) represents the net extraction reaction, whereas Eqs. (20) and (35) describe the extraction in detail, and enable the mechanistic modeling of the extraction process.

In order to study the extraction equilibrium of ammonia in the pH 2–10 range, the aqueous speciation reactions shown in Table 2 were considered, following the approach presented by Inoue et al. [30]. The value of the dissociation constant of ammonium nitrate was taken from Mozurkewich (1993) [35], whereas the rest of the constants were taken from the database of Medusa software [31].

2.2. Numerical methods

The model for the liquid–liquid extraction equilibrium of Co, Ni, and Li consists of nonlinear algebraic equations for the equilibrium constants of all the aqueous speciation reactions (Eqs. (1–18)), and the reactions in the assumed extraction mechanism (Eqs. (23), (25), (27), (29), (31), (34), (36)). In the same manner, the model for the liquid–liquid distribution equilibrium of ammonia consists of equations for the aqueous speciation reactions (Eqs. (37)–(40)), and the reactions in the assumed extraction mechanism (Eqs. (34) and (36)). In addition, the mass balance and electrical charge balance equations are needed to solve the systems of nonlinear algebraic equations for the equilibrium phase composition. The set of equations can be solved since it is possible to formulate the same number of independent equations as there are variables (species). However, a good initial guess is required, since otherwise erroneous or inaccurate results can be obtained. Therefore, a rate-based approach, described in the following section, is used herein as an alternative.

Solution of the phase equilibrium model

A rate-based approach [24,25,36] was used herein to solve the model equations, since the approach was found to be more efficient in comparison to the solution of a system of nonlinear algebraic equations using, for example, a Newton-Raphson method. The rate-based approach implies conversion of the nonlinear algebraic equations of the equilibrium constants and linear balance equations into the system of ordinary differential equations (ODEs). Since reversible chemical reactions proceed until an equilibrium is reached, the solution of a system of ODEs at plateau gives the same result as the solution of the respective system of nonlinear algebraic equations. Therefore, the element balance equations for the aqueous phase species, Eqs. (41), and the total mass balance equations, Eq. (42), for the heterogeneous two–phase reactions in a batch reactor can be used to calculate the composition of the process phases at equilibrium.

$$\frac{da_i^{Aq}}{dt} = -\sum_{j=1}^{S} \vartheta_{ij} R_j \quad (41)$$

$$\vartheta_{kj}\frac{da_k^{Org}}{dt} = -\vartheta_{ij}\frac{V_{Aq}}{V_{Org}}\frac{da_i^{Aq}}{dt} \quad (42)$$

where V_{Aq} and V_{Org} are the volumes of the aqueous and organic phases

respectively, t is the time, i is the index of species in the aqueous phase, k is the index of the corresponding species in the organic phase, j is the index of equilibrium reactions, S is the number of reactions in the system; ϑ is the stoichiometric coefficient of the species and R_j is the rate of an elementary reaction.

For an elementary reaction, Eq. (43), a reaction rate equation, Eq. (44), is formed directly from the reaction stoichiometry, in agreement with the mass action law. The reaction equilibrium constant, Eq. (45), gives a relationship between the forward and backward parts of the reversible reactions. The forward reaction rate constant can be assigned the value $k_f = 1000$. It can be the same for all the reactions, since it does not affect equilibrium but the time required to reach it.

$$\alpha A + \beta B + ... \rightleftarrows \gamma C + \delta D + ... \tag{43}$$

$$R_j = k_{f,j}(a_A^{\alpha} a_B^{\beta} \cdots - a_C^{\gamma} a_D^{\delta}/K_j) \tag{44}$$

$$K_j = \frac{k_{f,j}}{k_{r,j}} \tag{45}$$

where k_f and k_r are the reaction rate constants of the forward and backward reactions, respectively, K is the equilibrium constant.

The ODEs in Eqs. (41) and (42) can be solved simultaneously as an initial value problem by integration. In such a way, the model can be solved faster, at the same time the accuracy of the solution can be easily controlled by solver settings. The model was solved numerically using ode15s solver in Matlab.

Estimation of parameter values

All modeling in the current study was done in Matlab. An open source MCMC code package, developed by Laine [37,38], was used to estimate the reliability of the modeling results. The model developed for the liquid–liquid extraction equilibrium of Co, Ni, and Li was calibrated with the data presented by Virolainen et al. [6]. The unknown model parameters, *i.e.* the extraction equilibrium constants (Eqs. (23), (25), (27), (29), (31)), were estimated by nonlinear regression fitting of the experimentally measured extent of extraction of the metals, minimizing the sum of the squared residuals (Eq. (46)):

$$SSR_1 = \sum_{m=1}^{T} \sum_{j=1}^{N} (E_{m,j}^{exp} - E_{m,j}^{mod})^2 \tag{46}$$

where SSR is the sum of the squared residuals, E is the extent of metal extraction, j is the index of an experimental data point, N is the total number of experimental points, m is the number of a metal, and T is the total number of metals.

The model for the liquid–liquid extraction equilibrium of Co, Ni, and Li contains equilibrium constants for the ammonia liquid − liquid equilibrium distribution (Eqs. (34) and (36)). The constants were estimated separately, from independent data retrieved from Inoue et al. [30]. The extraction equilibrium constants (Eqs. (34) and (36)) were estimated by nonlinear regression fitting of logarithmic total concentration of ammonia in the organic phase, minimizing the sum of the squared residuals (Eq. (47)).

$$SSR_2 = \sum_{j=1}^{N} (Log([NH_4^+]_{org})_j^{exp} - Log([NH_4^+]_{org})_j^{mod})^2 \tag{47}$$

where j is the index of experimental points, and N is the total number of experimental points.

Process simulation

The process simulations were done using a sequential modular simulation approach. In the approach, the process step models are solved in the sequence in which the steps appear in the process under the condition, that the inlet stream compositions and flowrates are regulated. In the processes with the recirculating streams, the models of the interconnected steps are solved iteratively, until the mass balance over the entire process converges. The model developed in Section 2.1 is used to simulate loading, scrubbing and stripping stages in a continuous counter-current liquid–liquid extraction process.

3. Results and discussion

The model for the liquid − liquid extraction equilibrium of Co, Ni, and Li from a sulfate solution, developed in the current study, accounts for the extraction of ammonium along with the extraction of the metals. The models for ammonium equilibrium distribution and extraction of Co, Ni, and Li are first calibrated and then validated below. Finally, the main task, analysis of the separation process operation with different leachates is presented.

3.1. Model calibration

3.1.1. Ammonia equilibrium distribution

The extraction reaction equilibrium constants for ammonium shown in Eqs. (34) and (36), $K_{LLX}^{NH_4A(HA)_4}$ and $K_{LLX}^{NH_4A}$, were fitted against the data retrieved from Inoue et al. [30] minimizing the sum of the squared residuals in Eq. (47). The estimated values of the model parameters are presented in Table 3. The estimated value of $K_{LLX}^{NH_4A(HA)_4}$ differs from the value estimated by Inoue et al. [30]. This difference may result from the different approaches used for parameter estimation. The nonlinear regression modeling used herein is considered superior to linear regression, since linearization alters the error structure of the data.

The model developed in the current study shows an excellent fit (Fig. 2a) to the experimental data presented by Inoue et al. [30]. In comparison to the model of Inoue et al. [30], the model developed herein explains well the extraction behavior from acidic to basic solutions (pH 2–10).

3.1.2. Extraction equilibrium of Co, Ni, and Li

The model for calculating the compositions at phase equilibrium in the liquid − liquid extraction of Co, Ni, and Li from a sulfate solution using Cyanex 272 extractant was developed as described in Section 2.1. The parameters were fitted against the pH-extraction isotherms from Virolainen et al. [6] minimizing the sum of the squared residuals in Eq. (46). The composition of the sulfate leachate was 14 g/L Co, 0.5 g/L Ni, and 2.8 g/L Li. The estimated values of the model parameters, extraction equilibrium constants for Co, Ni, and Li, are presented in Table 3. The values of the model parameters were estimated for 1 M Cyanex 272 modified with 5% v/v trioctylamine (TOA). The modifier was used for decreasing organic-phase viscosity, and preventing third phase formation at high loading. The goodness of fit presented in Fig. 2b indicates a good correlation of the experimental data with the developed model.

The results of the MCMC analysis of the model parameters are presented in Fig. 3, which shows two-dimensional posterior distributions. The density of the dots in each subfigure represents the

Table 3
Estimated values of the parameters in the models for ammonia equilibrium distribution and extraction equilibrium of Co, Ni, and Li.

	log K	log σ[a]
$K_{LLX}^{NH_4A(HA)_4}$	−5.69	−6.20
$K_{LLX}^{NH_4A}$	−14.33	−14.46
$K_{LLX,1}^{Co}$	−6.43	−7.11
$K_{LLX,1}^{Ni}$	−9.97	−10.21
K_{LLX}^{Li}	−6.71	−6.92
$K_{LLX,2}^{Co}$	−2.28	−2.46
$K_{LLX,2}^{Ni}$	−0.72	−0.88

[a] The standard deviation of the parameter estimates was estimated using the Markov chain Monte Carlo method.

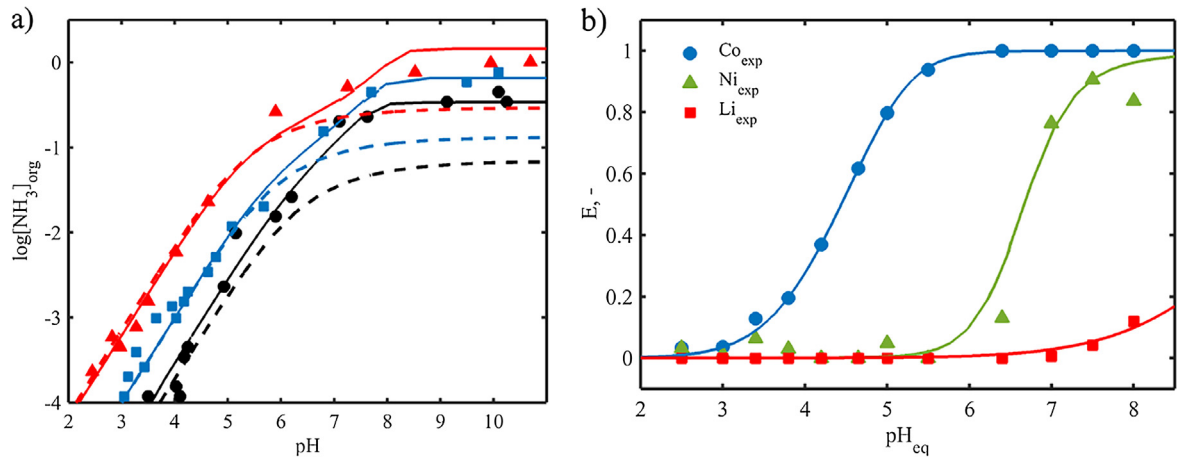

Fig. 2. (a) Extraction of ammonia with Cyanex 272. Total monomeric extractant concentration: ▲ = 1.45 M, ■ = 0.657 M, ● = 0.340 M. Experimental data from Inoue et al. [30]. Solid lines: prediction of the model from the current study, dashed lines: model from Inoue et al. [30]. (b) Dependence of metal extraction from the simulated sulfate leachate of Li-ion battery waste on the equilibrium pH. Symbols: circles = Co, triangles = Ni, squares = Li. Lines: model from the current study. Experimental data from Virolainen et al. [6].

probability that the true values of the parameters lie in that region, and the two circles represent the 95% and 90% probability regions of the parameters. It can be seen from the banana-shaped distribution in Fig. 3 that parameters $K^{Ni}_{LLX,1}$ and $K^{Ni}_{LLX,2}$ are slightly correlated. Such a correlation results from the small number of data points on the extraction isotherm for Ni in between pH 6 and 7, as the corresponding pair of parameters for Co does not correlate. All of the other parameters are well determined, as shown by the well-centered probability distributions, and the sharp peaks in the one-dimensional distributions. In addition, despite the correlation, the model with the fitted parameters explains the extraction of Co, Ni, and Li well, as can be seen in Fig. 2b.

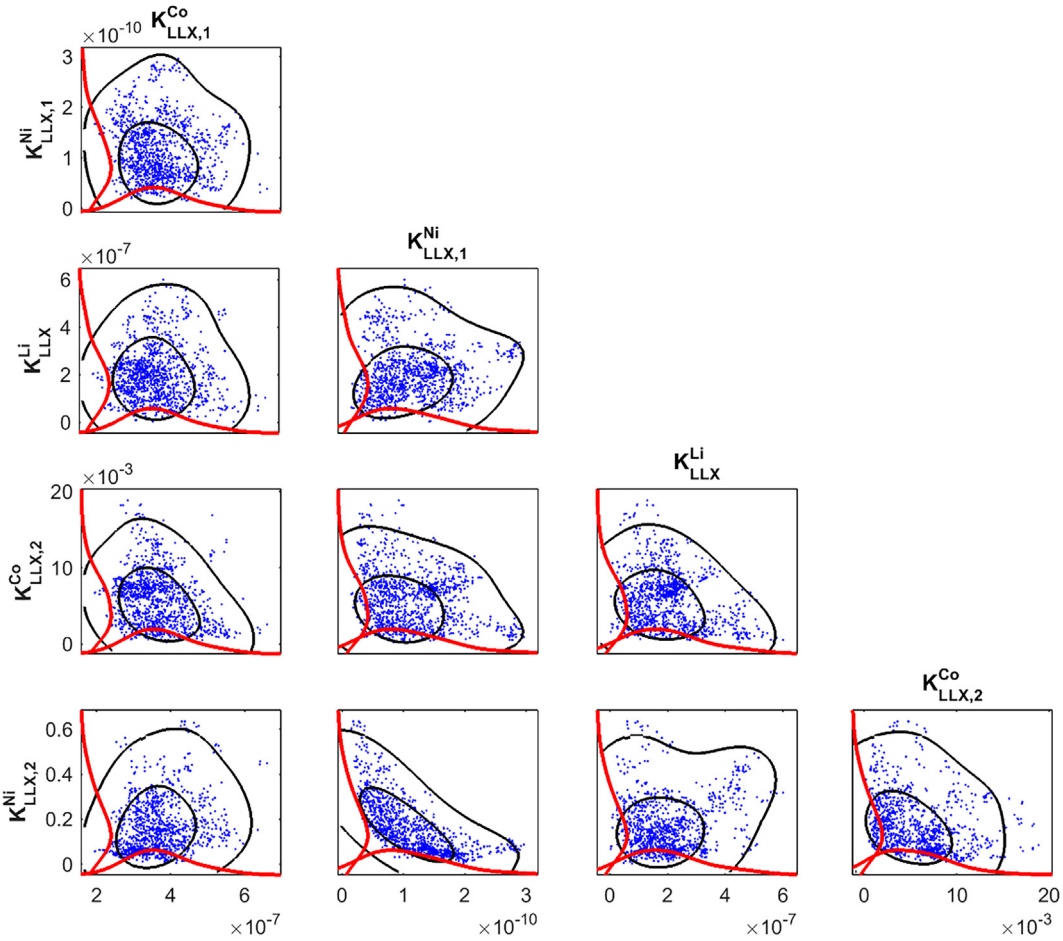

Fig. 3. Two-dimensional posterior distributions for the model parameters fitted with the data for the modified extractant. The 50% and 95% confidence regions (black lines), and the one-dimensional marginal densities (red lines), were calculated based on the density estimation. (For interpretation of the references to colour in this figure legend, the reader is referred to the web version of this article.)

3.2. Model validation

Once the equilibrium model parameters were estimated from the pH − extraction isotherms, the model was validated against experimental data on loading and stripping of the metals from Virolainen et al. [6]. The organic phase contained 1 M Cyanex 272 modified with 5% v/v TOA, and 48% pre-neutralized with ammonia, as presented by Virolainen et al. [6]. As can be seen in Figs. 4 and 5, the fitted model predicts well the loading and stripping equilibria.

From the excellent results of the predicted loading and stripping steps of the liquid − liquid extraction of Co, Ni, and Li, it was inferred that the model is also capable of predicting the scrubbing step in the process.

3.3. Separation process operation with different leachates

The model developed and validated above can be employed to design and analyze a continuous counter-current process for the separation of metals from Li-ion battery leachate. The common approach is to extract Co and Ni in separate liquid − liquid extraction circuits, whereas Li remains in the final raffinate after Ni extraction. For instance, such a process has been suggested in which both Co and Ni were produced as 99.9%, and Li as 99.8%, pure, using 2-ethylhexyl hydrogen(2-ethylhexyl)phosphonate (PC-88A) extractant [21,22]. Recently, Virolainen et al. [6] suggested a simplified flowsheet, in which Co and Ni were selectively extracted from the leachate with Cyanex 272, yielding pure Li raffinate. Co and Ni were consequently separated in the stripping stage and obtained as pure products. The loading, scrubbing, and stripping steps of the process were studied individually in equilibrium and bench-scale continuous counter-current separation experiments [6]. In the current numerical simulation study, this simplified and more efficient flow sheet is used to separate Co, Ni, and Li in a single process with loading, scrubbing, and two stripping steps (Fig. 6).

Since the leachates considered herein contain rather high concentrations of the metals, the extractant has to be partially neutralized to limit the release of protons in the loading stages, but this step is not explicitly considered here. Instead, the feed organic phase (PNO in Fig. 6), entering the loading step, is set to contain 1 M of Cyanex 272 with 5% v/v TOA, and is 48% pre-neutralized with ammonia.

The main difficulty in designing the process in Fig. 6 is the selection of appropriate operation parameters for the loading and scrubbing stages (O/A phase ratios and number of stages). This is because there is a recycling stream that feeds scrubbed Ni and Li back to the first loading stage. This interconnection makes performance of both of the stages interdependent.

The influence of the number of loading stages on the performance of the process is presented in Table 4. Here the leachate contains 14 g/L Co, 0.5 g/L Ni, and 2.8 g/L Li, and has a pH of 3.5. The scrubbing sulfate solution contains 0.3 g/L of Ni, and has a pH of 1.4. The O/A in loading and scrubbing were 0.57 and 1.00, respectively, in all simulations. The equilibrium pH of 7.5 was maintained in the last loading stage. The simulations show that the effect is minor and is mainly seen in Ni recovery. Using a single stage would yield low Li recovery and lower purity of Co and Ni in the loaded organic. Addition of the second loading stage resolved these issues. However, addition of a third stage makes the performance worse, since purity of Li in raffinate and recovery of Ni slightly drop. The cause of this drop is that the saponified extractant is consumed according to Eq. (20) in the last loading stages, whereas the extraction proceeds according to Eq. (32) in the first stage, where pH decreases, decreasing Ni extraction. The number of loading stages does not affect the Li recovery or its purity in the raffinate very much. Two loading stages appear to be the optimal process configuration, providing high recovery of Li, and loaded organic with high purity of Co and Ni. This result agrees well with the conclusion based on the experimental studies [6].

The influence of phase ratios on the performance of the interconnected loading (two stages) and scrubbing steps, with given feed composition and flow rate of the leachate, is presented in Fig. 7. Only the operation with O/A(scrubbing) < O/A(loading) is feasible here, due to the mass balance of the process streams. Fig. 7a shows the equilibrium pH in the second loading stage. It can be seen that the desired pH of around 7 is achievable within a narrow region only under the conditions studied. This requires a very stable process operation. The region where the pH is between 6.5 and 7.5 is marked in Fig. 7b–d with cyan and magenta lines. Fig. 7b shows that, when the process is operated such that pH 7 is maintained in the second loading step, the desired purity of Li (> 99%) in the raffinate is not achievable if the scrubbing product is recycled back to the loading feed. Instead, additional purification must be carried out by *e.g.* precipitation of lithium carbonate [7,39] or lithium phosphate [11,14]. Thereby a pure Li product can be achieved with the suggested liquid − liquid extraction process. Otherwise, pH around 7.5 can be adjusted by varying the O/A ratio in the second loading stage to increase Li purity in the raffinate, since concentrations of Co and Ni in the aqueous phase in this stage are such low that they are not precipitated. Fig. 7c demonstrates that operating the process at pH between 6.5 and 7.5 in the second extraction stage provides a pure mixture of Co and Ni in the scrubbed loaded organic phase.

Virolainen et al. [6] argued that keeping pH at around 6.5 in the scrubbing step provides complete scrubbing of Li leaving Ni and Co in the scrubbed loaded organic phase. The simulations of the interconnected loading and scrubbing steps, however, show (Fig. 7d) that

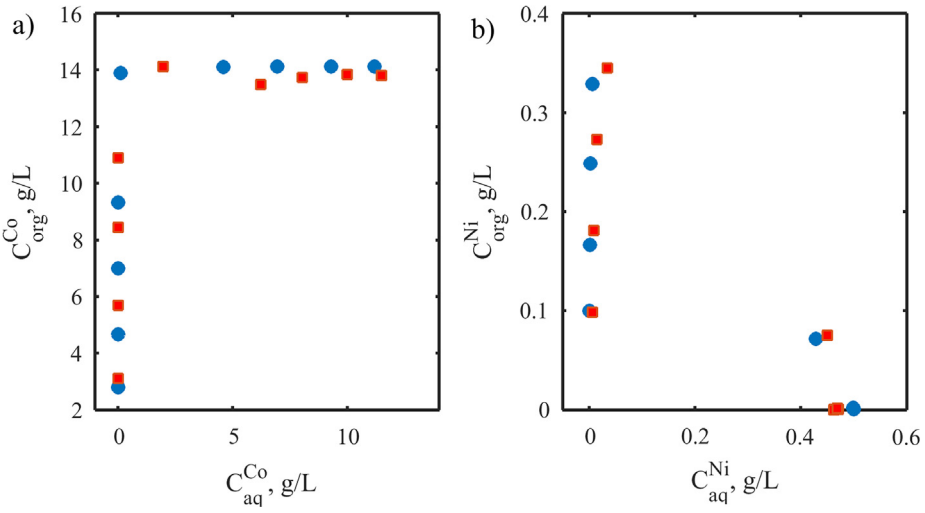

Fig. 4. Loading isotherms of (a) Co and (b) Ni for the 1 M Cyanex 272 modified with 5% TOA, used in the equilibrium experiments for the simulated sulfate leachate of Li-ion battery waste. Squares: experimental results, circles: modeling results. The equilibrium pH was not controlled. Experimental data is from Virolainen et al. [6].

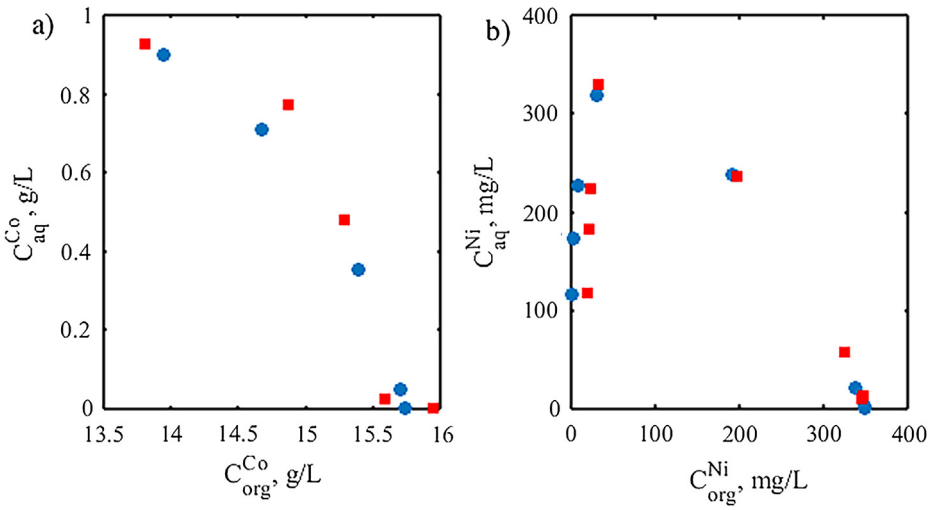

Fig. 5. Stripping isotherms of (a) Ni and (b) Co, with 0.025 M H_2SO_4 solutions from the 1 M Cyanex 272 modified with 5% TOA. Squares: experimental results, circles: modeling results. Equilibrium pH was not controlled. The experimental data is from Virolainen et al. [6].

this process scheme does not allow maintaining the equilibrium pH > 6 in the scrubbing stage, when pH is between 6.5 and 7.5 in the last loading stage. As a result, Ni is partially scrubbed along with Li. Therefore, some amount of Ni always circulates between the loading and scrubbing stages, decreasing the efficiency of extractant utilization. The low recovery of Ni (< 93%) in the simulations presented in Table 4 is explained by the same reason.

The recovery of Ni in the two-stage process can be improved by dosing a base to the first loading stage, which can decrease the required degree of neutralization of the PNO to the second loading stage. Even though part of the Ni is lost to the raffinate in the two-stage process in Table 4, the purity of the Li in the raffinate is very high (99.54%). This is due to the low concentration of Ni in the leachate (0.5 g/L) and the high equilibrium pH of 7.5 in the second loading stage. Low amounts of Co and Ni in the raffinate also decrease the risk of precipitation.

The performance (simulation results) of the interconnected loading and scrubbing stages of the processes with varying leachate composition is presented in Table 5. The O/A ratio in the scrubbing was set to 1 in all simulations, while the O/A in the two-stage loading step was adjusted so that the equilibrium pH of 7.5 maintained in the second loading stage. The same scrubbing solution (0.3 g/L Ni and pH 1.4) was used in all the processes. The simulations show very good performance of the processes with different leachate compositions when the equilibrium pH of 7.5 is maintained in the last loading stage by adjustment of

Table 4
Performance of the interconnected loading and scrubbing stages depending on the number of the loading stages.

Loading Stages	P^{Raff}_{Li}, %	R^{Raff}_{Li}, %	P^{LO}_{Co+Ni}, %	R^{LO}_{Co}, %	R^{LO}_{Ni}, %
1	99.72	99.86	99.78	100.00	92.76
2	99.54	99.99	99.99	100.00	88.06
3	99.42	99.99	99.99	100.00	84.55

O/A phase ratios in the loading and scrubbing stages. Co is recovered completely from the leachates into the LO, and most of the Li (> 99%) is left in the raffinate. At the same time, complete recovery of Ni is not achieved (due to low pH in the first loading stage as discussed above) with the highest recovery corresponding to the leachates II and III that have the highest Ni concentration. The higher recovery of Ni is followed by the lower purity of Li in the raffinate. However, the underlying reason is the higher Ni concentration in the leachates. It is thus concluded that higher Ni content of leachate impedes pure Li recovery in the process.

The performance of the separation process with the different leachate compositions in Table 5 is shown in Fig. 8. As seen in the figure, a purity of > 99% of Li in the raffinate is achieved with different O/A ratios for different leachates. Also the location of the feasible operating window (cyan and magenta lines) depends on the leachate composition.

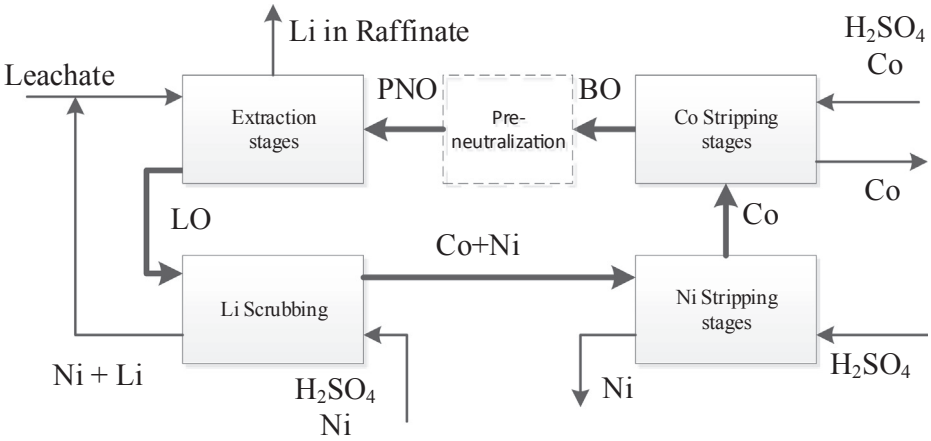

Fig. 6. Flowsheet for the continuous counter-current solvent extraction fractionation of metals in Li-ion battery waste leachate. LO = loaded organic, BO = barren organic, PNO = pre-neutralized organic. Thick and thin lines show organic and aqueous streams, respectively.

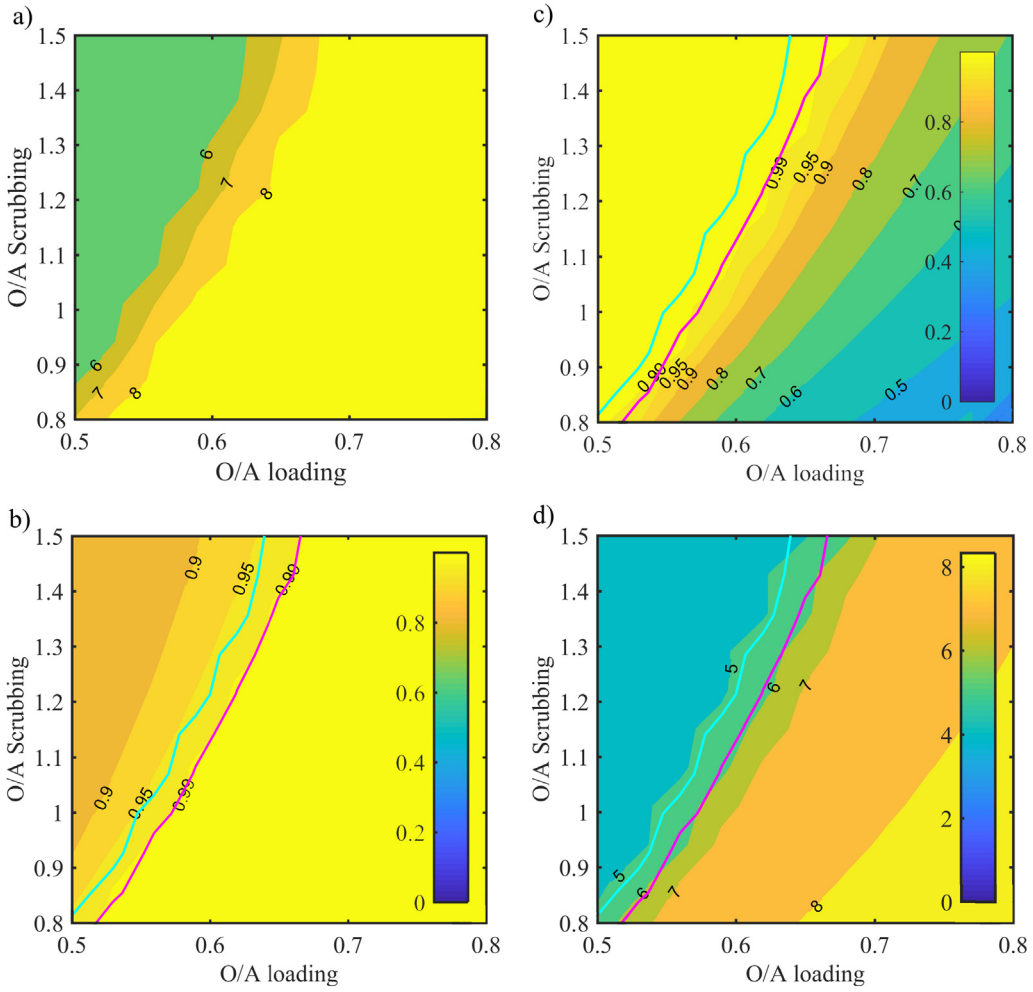

Fig. 7. Performance of the interconnected loading and scrubbing stages for the process with leachate I in Table 5 (a) Equilibrium pH in 2nd extraction step; (b) purity of Li in raffinate; (c) purity of Co and Ni together in the scrubbed loaded organic phase; and (d) equilibrium pH in the scrubbing step. The region with equilibrium pH in the second extraction step between 6.5 and 7.5 is between the cyan and magenta lines. (For interpretation of the references to colour in this figure legend, the reader is referred to the web version of this article.)

The leachates with higher total concentration of Co and Ni (Leachate II, III, and IV), require higher O/A ratio in the loading stage for the same O/A ratio in scrubbing.

Performance of the two-stage stripping of Ni from the loaded organic phases corresponding to the four cases in Table 5 is shown in Fig. 9. The loaded organic phase contains 11 g/L Co, O/A = 1. The stripping efficiency increases with increasing strip liquor acidity. The complete stripping of Ni is possible only at the cost of co-stripping of Co and, consequently, reduced Ni purity. The achievable Ni purity in the loaded strip liquor increases with the Ni concentration in the LO. If the Ni concentration in the LO is lower than 2 g/L, which is the case in Leachate I and Leachate IV, it is not possible to reach high Ni purity (> 99%) in strip liquor. Therefore, Leachates II and III with higher Ni concentrations are particularly well suited for this process since the product strip liquor with high Ni purity can be produced. Complete stripping of Co from the loaded organic after Ni stripping can be easily accomplished in one stage, for example, with a strip feed of 10 g/L Co and 25 g/L H_2SO_4 [29].

4. Conclusions

The influence of leachate composition on operation and performance of solvent extraction circuits for recovery and purification of Li, Co, and Ni from spent Li-ion battery leachates was studied by numerical simulations. For this purpose, a new model for the equilibrium of the liquid – liquid extraction of these metals from a sulfuric acid solution with bis(2,4,4-trimethylpentyl)phosphinic acid (Cyanex 272 extractant) was developed and validated. The model accounts for the aqueous phase speciation of the species present in the sulfate solution, and explains the extraction of the metal ions with Cyanex 272 by interfacial

Table 5
Performance (simulation results) of the interconnected loading and scrubbing stages of the processes with varying leachate composition.

Leachate	Co, g/L	Ni, g/L	Li, g/L	Source	O/A loading	P_{Li}^{Raff}, %	R_{Li}^{Raff}, %	P_{Co+Ni}^{LO}, %	R_{Co}^{LO}, %	R_{Ni}^{LO}, %	c_{Ni}^{LO}, g/L
I	14.0	0.5	2.8	[6]	0.57	99.57	99.99	99.98	100	88.59	0.62
II	16.7	11.0	1.4	[26]	0.72	98.48	99.95	99.98	100	98.45	4.59
III	11.3	11.5	1.8	[27]	0.67	98.98	99.94	99.96	100	98.73	5.76
IV	25.1	2.5	6.2	[21]	0.72	99.65	99.98	99.96	100	94.37	1.25

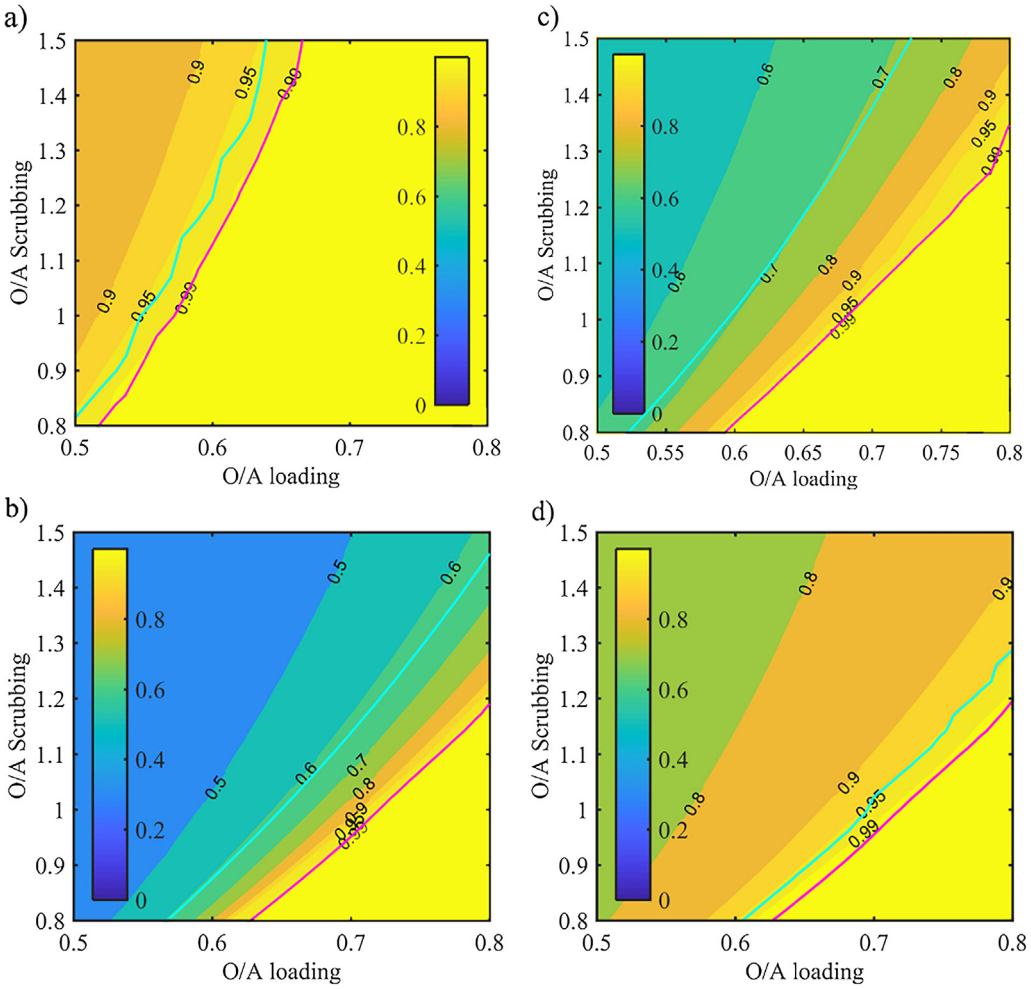

Fig. 8. Purity of Li in the raffinate, and the region where the equilibrium pH in the second extraction step is between 6.5 and 7.5 for the processes with different leachate compositions (Table 5). (a) Leachate I; (b) Leachate II; (c) Leachate III; and (d) Leachate IV.

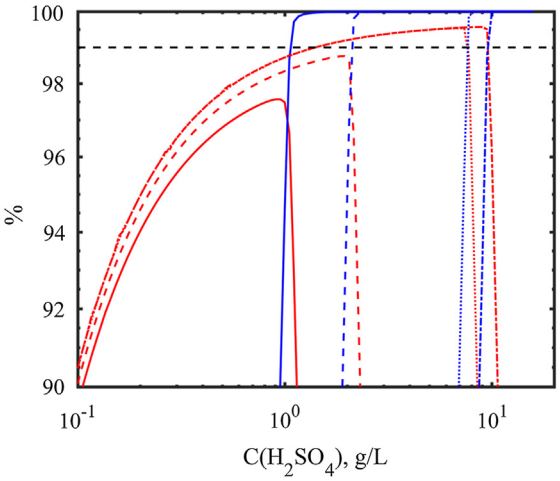

Fig. 9. Performance of the two-stage stripping of Ni from loaded organic with variable Ni concentration. Red: the purity of Ni in loaded strip liquor; blue: the stripping efficiency of Ni; black dashed line: 99% stripping efficiency. Ni concentration in loaded organic: solid line = Leachate I; dashed line = Leachate IV; dotted line = Leachate II; dash-dot line = Leachate III. (For interpretation of the references to colour in this figure legend, the reader is referred to the web version of this article.)

competitive ion exchange reactions of different stoichiometries. In addition, ammonium equilibrium distribution in the extraction system was modeled to enable prediction of the metal extraction with the pre-neutralized extractant.

The process flowsheet, in which Co and Ni are recovered together from the leachate in the loading step, leaving Li in the raffinate and where, subsequently, Co and Ni are separated and purified in the selective stripping step, was found to be very flexible. The process was shown to be applicable to separate Co, Ni, and Li from leachates of different composition. The process can be tuned for treatment of different leachates by adjustment of O/A phase ratios in the loading and scrubbing stages. It was found that high Ni content of the leachate impedes pure Li recovery in the process. The higher the Ni concentration in leachate, the higher purity of Ni is obtained in the stripped fraction. The process scheme allows adjusting the process performance to the changing market value of the metals.

References

[1] B. Swain, Recovery and recycling of lithium: a review, Sep. Purif. Technol. 172 (2017) 388–403, https://doi.org/10.1016/j.seppur.2016.08.031.
[2] A. Chagnes, B. Pospiech, A brief review on hydrometallurgical technologies for recycling spent lithium-ion batteries, J. Chem. Technol. Biotechnol. 88 (7) (2013) 1191–1199, https://doi.org/10.1002/jctb.4053.
[3] T. Träger, B. Friedrich, R. Weyhe, Recovery concept of value metals from automotive lithium-ion batteries, Chem. Ing. Tech. 87 (11) (2015) 1550–1557, https://doi.org/10.1002/cite.201500066.
[4] J.B. Goodenough, K.-S. Park, The Li-ion rechargeable battery: a perspective, J. Am. Chem. Soc. 135 (4) (2013) 1167–1176, https://doi.org/10.1021/ja3091438.

[5] A.A. Nayl, M.M. Hamed, S.E. Rizk, Selective extraction and separation of metal values from leach liquor of mixed spent Li-ion batteries, J. Taiwan Inst. Chem. Eng. 55 (2015) 119–125, https://doi.org/10.1016/j.jtice.2015.04.006.
[6] S. Virolainen, M. Fallah Fini, A. Laitinen, T. Sainio, Solvent extraction fractionation of Li-ion battery leachate containing Li, Ni, and Co, Sep. Purif. Technol. 179 (2017) 274–282, https://doi.org/10.1016/j.seppur.2017.02.010.
[7] R. Wang, Y. Lin, S. Wu, A novel recovery process of metal values from the cathode active materials of the lithium-ion secondary batteries, Hydrometallurgy 99 (3) (2009) 194–201, https://doi.org/10.1016/j.hydromet.2009.08.005.
[8] S. Ojanen, M. Lundström, A. Santasalo-Aarnio, R. Serna-Guerrero, Challenging the concept of electrochemical discharge using salt solutions for lithium-ion batteries recycling, Waste Manage doi: https://doi.org/10.1016/j.wasman.2018.03.045.
[9] X. Wang, G. Gaustad, C.W. Babbitt, Targeting high value metals in lithium-ion battery recycling via shredding and size-based separation, Waste Manage. 51 (2016) 204–213, https://doi.org/10.1016/j.wasman.2015.10.026.
[10] X. Chen, H. Ma, C. Luo, T. Zhou, Recovery of valuable metals from waste cathode materials of spent lithium-ion batteries using mild phosphoric acid, J. Hazard. Mater. 326 (2017) 77–86, https://doi.org/10.1016/j.jhazmat.2016.12.021.
[11] X. Chen, T. Zhou, J. Kong, H. Fang, Y. Chen, Separation and recovery of metal values from leach liquor of waste lithium nickel cobalt manganese oxide based cathodes, Sep. Purif. Technol. 141 (2015) 76–83, https://doi.org/10.1016/j.seppur.2014.11.039.
[12] X. Zeng, J. Li, N. Singh, Recycling of spent lithium-ion battery: a critical review, Crit. Rev. Environ. Sci. Technol. 44 (10) (2014) 1129–1165, https://doi.org/10.1080/10643389.2013.763578.
[13] G. Granata, E. Moscardini, F. Pagnanelli, F. Trabucco, L. Toro, Product recovery from Li-ion battery wastes coming from an industrial pre-treatment plant: Lab scale tests and process simulations, J. Power Sources 206 (2012) 393–401, https://doi.org/10.1016/j.jpowsour.2012.01.115.
[14] X. Chen, B. Xu, T. Zhou, D. Liu, H. Hu, S. Fan, Separation and recovery of metal values from leaching liquor of mixed-type of spent lithium-ion batteries, Sep. Purif. Technol. 144 (2015) 197–205, https://doi.org/10.1016/j.seppur.2015.02.006.
[15] D.S. Flett, Solvent extraction in hydrometallurgy: The role of organophosphorus extractants, J. Organomet. Chem. 690 (10) (2005) 2426–2438, https://doi.org/10.1016/j.jorganchem.2004.11.037.
[16] G.M. Ritcey, Solvent Extraction : Principles and Applications to Process Metallurgy. 2, G.M. Ritcey & Associates, cop., 2006, 2006.
[17] K. Sarangi, B.R. Reddy, R.P. Das, Extraction studies of cobalt (II) and nickel (II) from chloride solutions using Na-Cyanex 272, Hydrometallurgy 52 (3) (1999) 253–265, https://doi.org/10.1016/S0304-386X(99)00025-0.
[18] B. Swain, J. Jeong, J. Lee, G. Lee, Separation of cobalt and lithium from mixed sulphate solution using Na-Cyanex 272, Hydrometallurgy 84 (3) (2006) 130–138, https://doi.org/10.1016/j.hydromet.2006.03.061.
[19] R. Torkaman, M. Asadollahzadeh, M. Torab-Mostaedi, M. Ghanadi Maragheh, Recovery of cobalt from spent lithium ion batteries by using acidic and basic extractants in solvent extraction process, Sep. Purif. Technol. 186 (2017) 318–325, https://doi.org/10.1016/j.seppur.2017.06.023.
[20] P.E. Tsakiridis, S. Agatzini-Leonardou, Process for the recovery of cobalt and nickel in the presence of magnesium from sulphate solutions by Cyanex 272 and Cyanex 302, Miner. Eng. 17 (7) (2004) 913–923, https://doi.org/10.1016/j.mineng.2004.03.010.
[21] V.T. Nguyen, J.C. Lee, J. Jeong, B.S. Kim, B.D. Pandey, Selective recovery of cobalt, nickel and lithium from sulfate leachate of cathode scrap of Li-ion batteries using liquid-liquid extraction, Met. Mater. Int. 20 (2) (2014) 357–365, https://doi.org/10.1007/s12540-014-1016-y.
[22] V.T. Nguyen, J.C. Lee, J. Jeong, B.S. Kim, B.D. Pandey, The separation and recovery of nickel and lithium from the sulfate leach liquor of spent lithium ion batteries using PC-88A, Korean Chem. Eng. Res. 53 (2) (2015) 137–144, https://doi.org/10.9713/kcer.2015.53.2.137.
[23] C. Bourget, M. Soderstrom, B. Jakovljevic, J. Morrison, Optimization of the design parameters of a CYANEX 272 circuit for recovery of nickel and cobalt, Solvent Extr. Ion Exch. 29 (5–6) (2011) 823–836, https://doi.org/10.1080/07366299.2011.595640.
[24] F. Vasilyev, S. Virolainen, T. Sainio, Modeling the phase equilibrium in liquid–liquid extraction of copper over a wide range of copper and hydroxyoxime extractant concentrations, Chem. Eng. Sci. 171 (2017) 88–99, https://doi.org/10.1016/j.ces.2017.05.003.
[25] F. Vasilyev, S. Virolainen, T. Sainio, Modeling the liquid–liquid extraction equilibrium of iron (III) with hydroxyoxime extractant and equilibrium-based simulation of counter-current copper extraction circuits, Chem. Eng. Sci. 175 (2018) 267–277, https://doi.org/10.1016/j.ces.2017.10.003.
[26] J. Nan, D. Han, M. Yang, M. Cui, X. Hou, Recovery of metal values from a mixture of spent lithium-ion batteries and nickel-metal hydride batteries, Hydrometallurgy 84 (1) (2006) 75–80, https://doi.org/10.1016/j.hydromet.2006.03.059.
[27] Y. Yang, S. Xu, Y. He, Lithium recycling and cathode material regeneration from acid leach liquor of spent lithium-ion battery via facile co-extraction and co-precipitation processes, Waste Manage. 64 (2017) 219–227, https://doi.org/10.1016/j.wasman.2017.03.018.
[28] E. Lindell, E. Jääskeläinen, E. Paatero, B. Nyman, Effect of reversed micelles in Co/Ni separation by Cyanex 272, Hydrometallurgy 56 (3) (2000) 337–357, https://doi.org/10.1016/S0304-386X(00)00076-1.
[29] W. Thomas, Solvent extraction, Mining Chemicals Handbook (2010) 322–391.
[30] K. Inoue, D. Nakayama, Y. Watanabe, Extraction equilibria of ammonia with acidic organophosphorus compounds, Hydrometallurgy 16 (1) (1986) 41–53, https://doi.org/10.1016/0304-386X(86)90050-2.
[31] I. Puigdomenech, Chemical Equilibrium Diagrams, < https://sites.google.com/site/chemdiagr/ > , 2016 (Accessed 2017).
[32] J.M. Casas, V.G. Papangelakis, H. Liu, Performance of three chemical models on the high-temperature aqueous $Al_2(SO_4)_3$-$MgSO_4$-H_2SO_4-H_2O system, Ind. Eng. Chem. Res. 44 (9) (2005) 2931–2941, https://doi.org/10.1021/ie049535h.
[33] M.B. Mansur, M.J. Slater, E.C. Biscaia, Equilibrium analysis of the reactive liquid–liquid test system $ZnSO_4$/D2EHPA/n-heptane, Hydrometallurgy 63 (2) (2002) 117–126, https://doi.org/10.1016/S0304-386X(01)00211-0.
[34] D.P. Mantuano, G. Dorella, R.C.A. Elias, M.B. Mansur, Analysis of a hydrometallurgical route to recover base metals from spent rechargeable batteries by liquid–liquid extraction with Cyanex 272, J. Power Sources 159 (2) (2006) 1510–1518, https://doi.org/10.1016/j.jpowsour.2005.12.056.
[35] M. Mozurkewich, The dissociation constant of ammonium nitrate and its dependence on temperature, relative humidity and particle size, Atmos. Environ. Part A Gen. Top. 27 (2) (1993) 261–270, https://doi.org/10.1016/0960-1686(93)90356-4.
[36] T.O. Salmi, J.P. Mikkola, J.P. Wärnå, Chemical Reaction Engineering and Reactor Technology, CRC Press, Boca Raton, 2010.
[37] M. Laine, MCMC code package, < http://helios.fmi.fi/~lainema/mcmc/ > , 2017 (Accessed 2017).
[38] H. Haario, M. Laine, A. Mira, E. Saksman, DRAM: efficient adaptive MCMC, Stat. Comput. 16 (4) (2006) 339–354, https://doi.org/10.1007/s11222-006-9438-0.
[39] P. Zhang, T. Yokoyama, O. Itabashi, T.M. Suzuki, K. Inoue, Hydrometallurgical process for recovery of metal values from spent lithium-ion secondary batteries, Hydrometallurgy 47 (2) (1998) 259–271, https://doi.org/10.1016/S0304-386X(97)00050-9.